FEW-NUCLEON SYSTEMS: STATUS AND RESULTS OF INVESTIGATIONS

Yu.P. Lyakhno*

National Science Center "Kharkov Institute of Physics and Technology", 61108, Kharkov, Ukraine

(Received January 17, 2012)

The model-independent calculation of the nuclei ground state and the states of scattering can be carried out with due regard for realistic *NN* and 3*N* forces between nucleons and also, with the use of exact methods of solving the many-body problem. The tensor part of *NN* interaction and 3*NF*'s generate the lightest nuclei states with nonzero orbital momenta of nucleons. These states in the lightest nuclei are the manifestation of the properties of inter-nucleonic forces, and therefore, similar effects should be observed in all nuclei and also in all their excited states. In this paper primary attention is given to the investigation of the ^{4}He nucleus.

PACS: 25.10.+s; 23.20.-g

1. INTRODUCTION

From the physical standpoint, to describe the nucleon system, one must know the nucleon properties and also inter-nucleonic forces. The world constants and nucleon properties are known within sufficient accuracy, while inter-nucleonic forces are complicated in character and are known to a less accuracy. Unlike the atom, these forces cannot be described by the $1/r^2$ ratio (where r is the distance between nucleons) or by more complicated expressions like the Woods-Saxon potential [1]. The distinctive feature of inter-nucleonic forces is that they depend not only on the distance r, but also on the quantum configuration of the nucleon system, which is determined by the orbital momentum L, spin S and isospin T of this system.

The realistic *NN* potential can be determined phenomenologically from the experimental data on the ground state of the two-nucleon system and on the elastic (*p,p*), (*n,p*) and (*n,n*) scattering at nucleon energies up to 500 MeV. At higher nucleon energies, nonelastic processes come into play, and the potential approach becomes inapplicable. However, the data about the inter-nucleonic forces in this nucleon energy region are sufficient for the description of nuclear ground states, and also of nuclear reactions up to the meson-producing threshold.

The first phenomenological *NN* potentials were calculated relying on the analysis of relatively small arrays of the then existing experimental data on (*p,p*) and (*n,p*) scattering. Gammel and Thaller [2], using the data on differential cross-sections, nucleon polarization and the deuteron data, have calculated the central and tensor parts of *NN* potential, which were represented with the help of 14 adjustable parameters. The obtained results can also be represented as singlet and triplet phases of elastic nucleon scattering. In the further analyses, as the experimental data on (*p,p*) and (*n,p*) scattering were accumulated, adjustable expressions became more complicated, and the accuracy of *NN* potential calculations got improved. Among the most frequently used potentials, the Hamada-Johnston potential [3], Reid potential [4] and Paris potential [5] may be mentioned.

Nowadays, Argonne AV18 [6] and CD-Bonn [7] appear to be the most accurate potentials. In the construction of the charge-dependent CD-Bonn potential in the range of laboratory-system nucleon energies up to 350 MeV, 2932 (*p,p*)- and 3058 (*n,p*)-scattering data were used. Adjustable expressions were derived on the basis of the meson model of strong nucleon interactions. Account was taken of the π, ω and δ one-meson-exchange contribution, 2π -meson-exchange contribution, including Δ-isobar configurations, and also of the $\pi\rho$-exchange contribution. The quantity χ^2/datum was found to be 1.02 at number of adjustable parameters about 50. The results are presented in terms of *NN* phase-shift and mixing parameters. Table 1 gives the classification of two-nucleon system states.

Table 1. *Classification of two-nucleon system states. Boldface type denotes the states with the data available on them in the form of the CD-Bonn potential*

J	S=0		S=1	
	L-even	L-odd	L-even	L-odd
	T=1	T=0	T=0	T=1
0	$\mathbf{^1S_0}$			$\mathbf{^3P_0}$
1		$\mathbf{^1P_1}$	$\mathbf{^3S_1}$ + $\mathbf{^3D_1}$	$\mathbf{^3P_1}$
2	$\mathbf{^1D_2}$		$\mathbf{^2D_3}$	$\mathbf{^2P_3}$+$\mathbf{^2F_3}$
3		$\mathbf{^3F_1}$	$\mathbf{^3D_3}$+$\mathbf{^3G_3}$	$\mathbf{^3F_3}$
4	$\mathbf{^1G_4}$		$\mathbf{^3G_4}$	$\mathbf{^3F_4}$+$\mathbf{^3H_4}$
5		$^1H_5$	$^3G_5$ + $^3I_5$	$^3H_5$

*Corresponding author E-mail address: lyakhno@kipt.kharkov.ua

The following spectrometric notation is used for the purpose: $^{2S+1}L_J$, J is the total momentum of the system. The states, for which the dependence of NN interaction in the form of the CD-Bonn potential is obtained, are printed in bold type (up to $J \leq 4$). The total momentum J of the system may have even higher values, however with an increasing J the contribution of the states under decreases.

Arenhoevel *et al.* [8],[9] have calculated the structure functions of the reaction of polarized deuteron disintegration by polarized electrons with measurement of polarized nucleon recoil in different kinematic sectors. The measurement of these structure functions permits to separate out the contributions of π and ρ exchange, Δ-isobar configurations, and relativistic effects. This is of great importance for a more precise definition of the low-energy constants of meson-nucleon interaction.

At present, it is found that $3N$ forces take action in the nucleus. In the calculations, the $3N$ potentials of types UrbanaIX [10] and Tucson-Melbourne [11, 12] are most frequently used. Comparative study of three-nucleon force models are held in Ref. [13].

It is hoped, that the accuracy of measurements of realistic NN and NNN potentials would get further better, in particular, at the expense of using the data from double-polarization experiments [14]. A number of laboratories create polarized ^{3}He nuclear targets [15]-[17]. The investigation of disintegration of polarized ^{3}He nuclei by polarized beams of particles can provide some new information about $3N$ forces.

Along with the elaboration more precise definition of phenomenological potentials, important results were obtained through theoretical calculations of inter-nucleonic forces within the framework of chiral effective field theory (ChEFT). At present, the calculation of chiral interactions is not as accurate as that of phenomenological NN forces. Calculated within the framework of the ChEFT, the NN potential parameters for partial waves with $J \leq 3$ are in satisfactory agreement with the experiment in the region of nucleon lab energy up to $T_N \sim$290 MeV [18]. In the context of the ChEFT, Rozpedzik *et al.* [19] estimated the effect of $4N$ forces and found the additional contribution of $4N$ forces to the binding energy of the ^{4}He nucleus to be about several hundreds of keV.

The calculations in the context of ChEFT are of particular importance for explaining the origin and explicit representation of $3N$ and $4N$ forces. The reason is that there are a good many experimental data to determine the NN potential, whereas for determination of $3N$ and $4N$ forces these data are not nearly enough. The origin and the explicit form of $3N$ and $4N$ forces it is a basic issue of few-nucleon systems.

Mathematically, to describe the nucleon system, it is necessary to use the accurate methods of solving the many-nucleon problem. The solution of this problem is an intricate theoretical task. The method for solving the three-body problem in the limit of the zero radius of action has been proposed in Ref. [20]. To describe the three-body system in the case of an arbitrary two-body potential, Faddeev [21] suggested solving a set of connected integral equations. At negative energy of the particle system these equations are homogeneous, while at positive energy the equations are non-homogeneous. In a special case of three different spinless particles, the system comprises three equations. Should the particles have spins, then it is necessary to set up equations for each possible quantum configuration of the system. Later on, Yakubovsky [22] generalized this result for the case of any number of particles in the system.

In this connection, that $3N$ forces participation in the nucleus, for exact description of a many-nucleon system it is necessary to solve the set of connected integral equations with due regard for the contribution of NN and $3N$ forces. The solution of the problem by the Faddeev-Yakubovsky (FY) method was first reported by Gloeckle and Kamada (GK) [23].

The realistic NN and NNN forces were also used in the calculations by the Lorentz integral transform (LIT) method [24], [25] the hyperspherical harmonic variational method (HHVM) [26], the refined resonating group model (RRGM) [27], [28] and others [29].

Section 2 presents the results of theoretical calculations of the ground states of few-nucleon nuclei, and also, the examples of nuclear reaction calculations based on the realistic NN and NNN forces. Section 3 describes the results of the study into the ^{4}He nuclear structure, and also, presents the multipole analysis of the $^4\mathrm{He}(\gamma, p)\mathrm{T}$ and $^4\mathrm{He}(\gamma, n)^3\mathrm{He}$ reactions, performed on the basis of the experimental data about the differential cross-sections and cross-section asymmetry with linearly polarized photons. The possible effects, determined by realistic inter-nucleonic forces in nuclei with $A > 4$ are discussed in Section 4. The conclusions are formulated in Section 5.

2. RESULTS OF THE THEORETICAL CALCULATIONS

The characteristics of three- and four-nucleon systems by the FYGK method were calculated in works [30]-[34]. In Ref. [31] calculation of the ground-state of the α-particle is carried out. The calculations took into account the contributions from the states of the NN system having the total momentum up to $J \leq 6$. The consideration of large total-momentum values of the two-nucleon system is necessary, for example, for a correct calculation of short-range correlations. In the calculation [31], account was taken of the states, in which the algebraic sum of orbital momenta of all nucleons of the ^{4}He nucleus was no more than l_{max}=14. The system comprised 6200 partial waves. The authors of work [31] estimated their mistake in the calculations of ^{4}He nuclear binding energy to be $\sim$50 keV. Considering that the calculated value of the binding energy is $\sim$200 keV higher than the experimental value, the authors have made a conclusion about a possible contribution of $4N$ forces that are of repulsive nature.

Table 2 lists the values of nuclear binding energies (in MeV) for ^{4}He, ^{3}H, ^{3}He and ^{2}H, calculated with the use of *NN* potentials AV18 and 3*NF*'s UrbanaIX. It is evident from the table that without taking into account the 3*N* forces, the nuclei appear underbound, while with due regard for the forces the agreement with experimental data is satisfactory.

Table 2. *Binding energies (in MeV units) of ^{4}He, of ^{3}H, of ^{3}He and of ^{2}H, calculated with Argonne V18 and Argonne V18 + Urbana IX interaction*

Inter-action	Method	^{4}He	^{3}H	^{3}He	^{2}H
AV18	FY	-24.28	-7.628	-6.924	
	RRGM	-24.117	-7.572	-6.857	-2.214
	HHVM	-24.25			
AV18+	FYKG	-28.50	-8.48	-7.76	
+UIX	RRGM	-28.342	-8.46	-7.713	-2.214
	HHVM	-28.50	-8.485	-7.742	
	Exp	-28.296	-8.481	-7.718	-2.224

Similar results were obtained with the use of the *NN* potential CD-Bonn and the 3*N* potential Tucson-Melbourne.

Table 3 gives the calculated root-mean-square radii r_{rms} of the ^{4}He nucleus [26, 28]. The agreement with experiment is also satisfactory.

Table 3. *The ^{4}He nucleus $< r^2 >^{1/2}$ radii (fm), where r-distance between nucleons centers*

Interaction	Method	^{4}He
AV18	RRGM	1.52
	HHVM	1.512
AV18+UIX	RRGM	1.44
	HHVM	1.43
	Exp	1.67

It should be also noted that the Coulomb interaction between protons results in the production of T=1 and T=2 isospin states of ^{4}He. Table 4 gives the probabilities of these states for the ^{4}He nucleus calculated in papers [26], [31].

Table 4. *Contribution of different total isospin states to the ^{4}He nuclear wave function. The values are given in %*

Interaction	Method	T=0	T=1	T=2
AV18	FY	99.992	$3{\cdot}10^{-3}$	$5{\cdot}10^{-3}$
	HHVM		$2.8{\cdot}10^{-3}$	$5.2{\cdot}10^{-3}$

The tensor part of *NN* interaction and 3*NF's* generate the ^{4}He nuclear states with nonzero orbital momenta of nucleons. The measurement of probability for $l \neq 0$ states occurrences provides new information about these properties of inter-nucleonic forces. For illustration, Table 5 gives possible ^{4}He nuclear states allowed by the laws of conservation of the total momentum and parity. The symbols s and l denote the spin and orbital momentum of the nucleon, respectively. According to the vector addition rules, spins and orbital momenta of individual nucleons are summed so that the total momentum J of the ^{4}He nucleus and its parity π are conserved and remain equal to 0^+. The nuclear shell model predicts only one state given in the first row of Table 5. The probability of this state has been calculated to be around 84%. The nuclear states of ^{4}He, listed in Table 5, satisfy the Pauli principle.

Table 5. *Scheme of possible quantum states of the ^{4}He nucleus*

States of the ^{4}He nucleus	p l,s	n l,s	p l,s	n l,s	L,S	J^π	P,%
$^1S_0$	0↑	0↑	0↓	0↓	0,0	0^+	84
	1↑	0↑	0↓	1↓	0,0	0^+	
	1↑	1↑	1↓	1↓	0,0	0^+	
	2↑	1↑	1↓	0↓	0,0	0^+	
	-	-	-	-			
$^3P_0$	1↑	0↑	0↑	1↓	1,1	0^+	0.7
	2↑	0↑	0↑	1↓	1,1	0^+	
	2↑	2↑	0↑	0↓	1,1	0^+	
	3↑	1↑	1↑	1↓	1,1	0^+	
	-	-	-	-			
$^5D_0$	0↑	0↑	1↑	1↑	2,2	0^+	16
	2↑	0↑	0↑	2↑	2,2	0^+	
	2↑	1↑	1↑	2↑	2,2	0^+	
	3↑	1↑	1↑	3↑	2,2	0^+	
	-	-	-	-			

Table 6 gives the probabilities of S, S', P and D states of the ^{4}He and ^{3}He nuclei calculated by Nogga *et al.* [31], where S' is a part of $^1S_0$-states with nonzero orbital momenta of nucleons. The calculations gave the probability of $^5D_0$ states having the total spin S=2 and the total nucleon orbital momentum L=2 of the ^{4}He nucleus to be $\sim$ 16%, and the probability of $^3P_0$ states having S=1, L=1 to be between 0.6 and 0.8%. It is obvious from Table 6 that the consideration of the 3*NF's* contribution increases the probability of $^3P_0$ states by a factor of $\sim$2.

Table 6. *S, S′, P, and D state probabilities for ^{4}He and ^{3}He*

	^{4}He				^{3}He			
Interaction	S%	S'%	P%	D%	S%	S'%	P%	D%
AV18	85.45	0.44	0.36	13.74	89.95	1.52	0.06	8.46
CD-Bonn	88.54	0.50	0.23	10.73	91.45	1.53	0.05	6.98
AV18+UIX	82.93	0.28	0.75	16.04	89.39	1.23	0.13	9.25
CD-Bonn+TM	89.23	0.43	0.45	9.89	91.57	1.40	0.10	6.93

2.1. STATES OF SCATTERING

A full calculation of the nuclear reaction must take into account the ground-state structure of the nucleus, the contribution of the interaction of the probe with nucleons and meson exchange currents (MEC), quantum configuration of the off particles and the final-state interaction of particles (FSI). These calculations were carried out for three-nucleon nuclei. In the work of Gloeckle *et al.* [35], the analysis of electron scattering by ^{3}He and ^{3}H nuclei was performed. Elastic charge F_{ch}(q) and magnetic F_m(q) form factors, inclusive electron scattering, pd-breakup and full-breakup of these nuclei were calculated with the use of the AV18 *NN* force and the Urbana IX $3NF$*'s*. The contribution of the π and ρ exchange was taken into account according to Riska's prescription [36]. The calculations were performed by the Faddeev scheme, that allowed one to analyze in detail the $3NF$*'s*, MEC and FSI contributions to different observable quantities. Fig. 1 shows the elastic charge F_{ch}(q) and magnetic F_m(q) form factors of the ^{3}He nucleus. The discrepancy between the calculation and the experiment at high-transfer momentum values (q>3 fm^{-1}) was attributed by the authors of [35] to the contribution of relativistic effects.

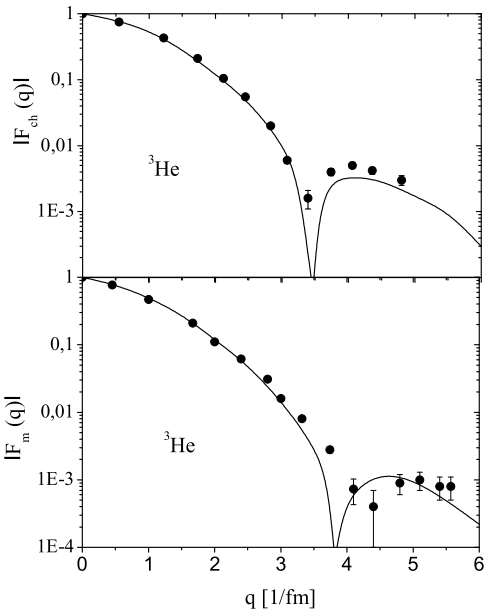

Fig.1. *Elastic charge $F_{ch}(q)$ and magnetic $F_m(q)$ form factors of the ^{3}He nucleus. The experimental data are taken from Ref.[37], the curve - from Ref.[35]*

Similar calculations were carried out for the radiative proton-deuteron capture reaction (Golak *et al.* [38], Kotlyar *et al.* [39]), three-nucleon photodisintegration of ^{3}He (Skibinski *et al.* [40]).

The calculations of nuclear reactions in ^{4}He nucleus were performed by the RRGM method [28] with using potentials AV18 and UrbanaIX, and with using semi-realistic potential [41], by the LIT method with realistic potentials [25] and with semi-realistic potential MT I-III [42], and also other methods. There is a dispersion between different theoretical calculations.

Theoretical calculations [27], [43] and numerous experiments were carried out to investigate hadronic probe reactions with participation of three and four nucleons [44], [45].

3. STRUCTURE IVESTIGATIONS OF ^{4}He BY MEANS OF PHOTOREACTIONS

For measuring the probability of $^5D_0$ states of the ^{4}He nucleus, it is reasonable to investigate the ^{2}H$(\vec{d},\gamma)^4$He reaction of radiative deuteron-deuteron capture. The tensor analyzing power of the reaction is sensitive to the contribution of $^5D_0$ states Weller *et al.* [46]-[48]. In these studies the differential cross section, the vector and tensor analyzing power of reaction measured in the deuteron energy range 0.7< E_d <15 MeV. In Ref. [48] was made a comparison of this data with theoretical calculation Wachter *et al.* [49]. The agreement of the calculation with the experiment was achieved in the assumption, that the probability $^5D_0$ states of the ^{4}He nucleus composes $\sim$ 2.2%. In this calculation the semi-realistic *NN* potential was used. In work Mellema *et al.* [50] has measured the differential cross-section, the vector and tensor analyzing powers of the reaction at the deuteron energy E_d=10 MeV. In fitting, the best agreement with the experimental data was obtained in the assumption that $^1D_2$(E2), $^5S_2$(E2), $^3P_1$(E1) and $^3P_2$(M2) were the basic transitions. The probability of the $^5D_0$ state of the ^{4}He nucleus was estimated around 15%. However, it is marked in this work that at the calculation of this probability there is a problem of account of the tensor-force effects in the incident channel which also contribute to the measured values of the multipole amplitudes. The reaction was investigated at the deuteron energy E_d =1.2 MeV [51], and also at E_d =20, 30 and 50 MeV [52].

At low deuteron energies, the $^5S_2(E2) \rightarrow {}^5D_0$ transition should dominate. This is due to the fact that at a low deuteron energy the $^1D_2(E2)$, $^5D_2(E2)$, $^5G_2(E2)$ and $^3F_2(M2)$ transitions are suppressed by the angular momentum barrier. The $^3P_1(E1)$ and $^3P_2(M2)$ transitions to the final state $^1S_0$ or $^5D_0$ are suppressed because of the spin flip ΔS=1 [28]. Besides, in the reaction under discussion the $E1$ and $M1$ transitions are suppressed according to the isospin selection rules for self-conjugate nuclei (ΔT=1) [53]. The analysis of measured differential cross section, vector/tensor analyzing powers of the reaction at the deuteron energy $E_{c.m.}$= 60 keV Sabourov *et al.* [54] has shown the transition probabilities to be $^5S_2(E2)$=(55±8)%, $^3P_1(E1)$=(29±6)% and $^3P_2(M2)$=(16±3)%. Significant cross sections for $^3P_1$(E1) and $^3P_2$(M2) transitions may be due to a greater contribution of $^3P_0$ states of the ^{4}He nucleus than it follows from the calculations [26, 31]. In turn, the last fact may be the result of a high sensitivity to the peculiarities of *NN* and $3N$ potentials

[31]. The contribution of meson exchange currents that may cause the spin flip ΔS=1 is also possible. In view of this, the experimental data obtained from the study of only one reaction appear insufficient for calculating the probabilities of states with nonzero orbital momenta of nucleons.

A new information about the $l \neq 0$ states of ^{4}He can be obtained from studies of the $^4\mathrm{He}(\gamma,p)^3\mathrm{H}$ and $^4\mathrm{He}(\gamma,n)^3\mathrm{He}$ reactions, and also, the reactions of radiative capture of protons or neutrons by tritium or ^{3}He nuclei, respectively. In this case, the transitions from $^3P_0$ states of the nucleus to the final S=1 state occur without any spin flip. So, it may be expected that the comparison between the *E1* and *M1* transition cross-sections in (d,γ) and (γ,N) reactions would provide new information on the contribution of MEC.

The first experimental data on spin-triplet transitions have been obtained from studies of the reaction of radiative capture of protons by tritium nuclei. When investigating the $^3\mathrm{H}(\vec{p},\gamma)^4\mathrm{He}$ reaction on a polarized protons beam of energies between 0.8 and 9 MeV, Wagenaar *et al.* [55] came to the conclusion that $^3S_1(M1)$ was the basic transition. At the same time, from the studies of the same reaction but at polarized protons energy E_p=2 MeV Pitts [56] has stated $^3P_1(E1)$ to be the basic transition. This reaction was investigated also at protons energy E_p=80 keV [57]. In this work the conclusion that a basic transition with the spin of S=1 is $^3S_1(M1)$. These contradictory statements are due to the fact that the experimental data obtained had significant errors. At higher energies, the measurements are complicated by the necessity of considering the amplitude $^3D_1(M1)$, which is suppressed at low photon energies by the angular momentum barrier.

Nowadays, were made more than ten experimental works on measurement total and differential cross-section reactions $^4\mathrm{He}(\gamma,p)^3\mathrm{H}$ and $^4\mathrm{He}(\gamma,n)^3\mathrm{He}$ in energies range at the giant dipole resonance peak. The results of these measurements can be found in the work Tornow *et al.* [58]). The data obtained by different laboratories on the total cross section these reactions attains a factor of ∼2.

To measurement the S=1 transition cross-sections for the reactions $^4\mathrm{He}(\gamma,p)^3\mathrm{H}$ and $^4\mathrm{He}(\gamma,n)^3\mathrm{He}$, one needs the experimental data about the cross sections of these reactions in the collinear geometry, and also the polarization observable quantities.

In Refs. [59, 60], chambers placed in the magnetic field were used to detect the reaction products. This has permitted measurements of the differential cross section of the reactions in the range of polar nucleon-exit angles $0^0 \leq \theta_N \leq 180^0$. However, the number of events registered in those experiments, was insufficient for measuring the reaction cross-sections in collinear geometry.

Jones *et al.* [61] have measured the differential cross section of the $^4\mathrm{He}(\gamma,p)^3\mathrm{H}$ reaction at the energy of tagged bremsstrahlung photons $63 \leq E_\gamma \leq 71$ MeV. The reaction products were registered by means of a large-acceptance detector LASA with electronic information retrieval. The measurements were performed in the interval of polar proton-exit angles $22.5^0 \leq \theta_N \leq 145.5^0$. The absence of the data at large and small angles has led to significant errors in the cross section measurements of this reaction in the collinear geometry.

Nilsson *et al.* [62] investigated the reaction $^4\mathrm{He}(\gamma,n)$ in the energy range of tagged bremsstrahlung photons $23 \leq E_\gamma \leq 70$ MeV. The time-of-flight technique was employed to determine the neutron energy. However, the measurements of this reaction at large and small angles were not performed either.

In the work Shima *et al.* [63] used a monoenergetic photon beam in the energy range from 21.8 to 29.8 MeV and nearly 4π time projection chamber, were measured the total and differential cross-sections for photodisintegration reactions of the ^{4}He nucleus. Authors received that the M1 strength is about (2±1)% of the E1 strength.

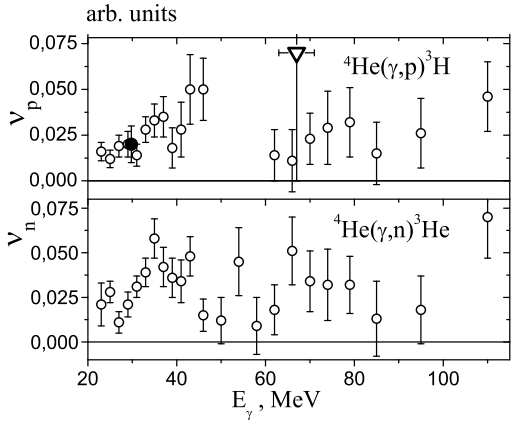

Fig.2. *The total cross-section in collinear geometry reactions $^4He(\vec{\gamma},p)T$ and $^4He(\vec{\gamma},n)^3He$. Triangle; Jones et al. [61], filled circle; Shima et al. [63], open circles; Nagorny et al. [66]. The errors are statistical only.*

Differential cross sections for two-body (γ,p) and (γ,n) reactions have been measured in works Arkatov *et al.* [64], [65] in the photon energy range from the reaction threshold up to E_γ=150 MeV. The reaction products were registered with the help of a diffusion chamber. Later, these data were processed for the second time in the work of Nagorny *et al.* [66]. The data are based on the statistics of $\sim 3 \cdot 10^4$ events in each of the (γ,p) and (γ,n) reaction channels. The cross sections were measured with a 1 MeV step up to E_γ=45 MeV, and with a greater step at higher energies, as well as with a 10^0 step in the polar nucleon-exit angle in the c.m.s. Unfortunately, authors published data about differential cross-sections only at photon's energies 22.5, 27.5, 33.5, 40.5, 45, and 49 MeV. As a result of multipole analysis Voloshchuk [67], the total cross sections for electric dipole and electric quadrupole transitions with the S=0 spin in the final state of the particle

system, and also, the phase shift between *E1* and *E2* amplitudes were calculated from the differential cross sections. The total cross-section in collinear geometry reactions ^{4}He$(\vec{\gamma},p)$T and ^{4}He$(\vec{\gamma},n)^3$He are shown in Fig. 2.

The angular dependence of cross-section asymmetry in the ^{4}He$(\gamma,p)^3$H and ^{4}He$(\vec{\gamma},n)^3$He reactions with linearly polarized photons of energies 40, 60 and 80 MeV was measured by Lyakhno *et al.* [68, 69]. The beam of linearly polarized photons was produced as a result of coherent bremsstrahlung of 500, 600 and 800 MeV electrons, respectively, in a thin diamond single crystal. The reaction products were registered with the use of a streamer chamber located in the magnetic field [70]. The observed data on the angular dependence of the cross-section asymmetry are presented in Fig. 3. Here the square represents the data obtained with semi-conductor detectors by the ΔE-E method [71]. The dashed curve is the calculation by Mel'nik and Shebeko [72] made in the plane-wave impulse approximation with consideration of the direct reaction mechanism and the mechanism of recoil.

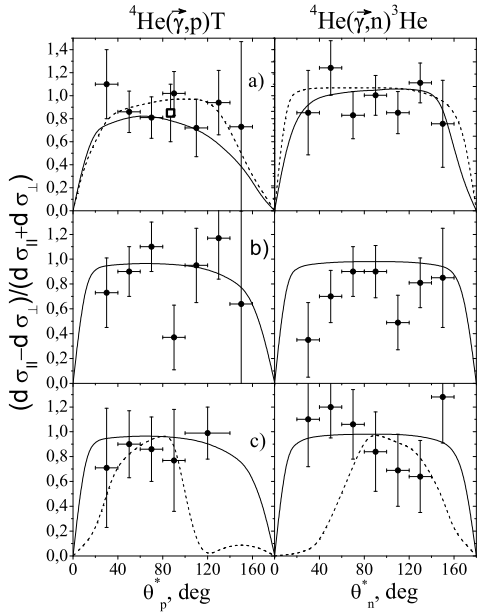

Fig. 3. *Angular dependence of cross-section asymmetry of linearly polarized photon reactions $^4He(\vec{\gamma},p)T$ and $^4He(\vec{\gamma},n)^3He$. The points represent the results of Refs. [68, 69]: a) E_γ^{peak}=40 MeV, b) E_γ^{peak}=60 MeV, c) E_γ^{peak}=80 MeV. The square shows the data of Ref. [71]. The errors are statistical. The solid curve - calculation [66], the dashed curve - calculation [72]*

It was indicated in Ref. [72] that without consideration of the mechanism of recoil the cross-section asymmetry in the $(\vec{\gamma},n)$ channel would be equal to zero. This is due to the fact that in the mentioned approximation the ^{4}He$(\gamma,n)^3$He reaction is contributed only by the magnetic component of the interaction Hamiltonian. So, the asymmetry $\Sigma(\theta_n)$ in the $(\vec{\gamma},n)$ channel measured in the experiment to be close to unity confirms an essential role of the mechanism of recoil. The solid curves represent the calculation [66] that meets the requirements of covariance and gauge invariance. The calculation took into account the contribution of a number of diagrams corresponding to the pole mechanisms in s-, t- and u-channels, the contact diagram c, and also a number of triangular diagrams. A satisfactory fit of the calculation to the experiment confirms an essential role of the direct reaction mechanism, the mechanism of recoil and the final-state rescattering effects.

3.1. MULTIPOLE ANALYSIS OF ^{4}He(γ,p)T AND ^{4}He$(\gamma,n)^3$He REACTIONS

In the *E1*, *E2* and *M1* approximations, the laws of conservation of the total momentum and parity for two-body (γ,p) and (γ,n) reactions of ^{4}He nuclear disintegration permit two multipole transitions $E1^1P_1$ and $E2^1D_2$ with the spin S=0 and four transitions $E1^3P_1$, $E2^3D_2$, $M1^3S_1$ and $M1^3D_1$ with the spin S=1 of final-state particles. The differential cross section in the c.m.s. can be expressed in terms of multipole amplitudes as follows [73, 74]:

$$\begin{aligned}\frac{d\sigma}{d\Omega} = \frac{\lambda\!\!\!^{-2}}{32}\{&\sin^2\theta[18|E1^1P_1|^2 - 9|E1^3P_1|^2\\ &+9|M1^3D_1|^2 - 25|E2^3D_2|^2\\ &-18\sqrt{2}Re(M1^3S_1^*\,M1^3D_1) + 30\sqrt{3}Re(M1^3D_1^*\,E2^3D_2)\\ &+30\sqrt{6}Re(M1^3S_1^*\,E2^3D_2)\\ &+\cos\theta(60\sqrt{3}Re(E1^1P_1^*\,E2^1D_2)\\ &-60Re(E1^3P_1^*\,E2^3D_2))\\ &+\cos^2\theta(150|E2^1D_2|^2 - 100|E2^3D_2|^2)]\\ &+\cos\theta[-12\sqrt{6}Re(E1^3P_1^*\,M1^3S_1)\\ &-12\sqrt{3}Re(E1^3P_1^*\,M1^3D_1) + 60Re(E1^3P_1^*\,E2^3D_2]\\ &+18|E1^3P_1|^2 + 12|M1^3S_1|^2 + 6|M1^3D_1|^2\\ &+50|E2^3D_2|^2 + 12\sqrt{2}Re(M1^3S_1^*\,M1^3D_1)\\ &-20\sqrt{6}Re(M1^3S_1^*E2^3D_2) - 20\sqrt{3}Re(M1^3D_1^*\,E2^3D_2)\}\,,\end{aligned} \tag{1}$$

where $\lambda\!\!\!^{-}$ is the reduced wavelength of the photon.

It is known that the cross-section asymmetry of the linearly polarized photon reaction is described by the following expression [69]:

$$\begin{aligned}\Sigma(\theta) = \sin^2\theta\{&18\mid E1^1P_1|^2 - 9|E1^3P_1|^2\\ &-9|M1^3D_1|^2 + 25|E2^3D_2|^2\\ &+18\sqrt{2}Re(M1^3S_1^*\,M1^3D_1) + 10\sqrt{3}Re(M1^3D_1^*\,E2^3D_2)\\ &+10\sqrt{6}Re(M1^3S_1^*\,E2^3D_2)\\ &+\cos\theta[60\sqrt{3}Re(E1^1P_1^*\,E2^1D_2)\\ &-60Re(E1^3P_1^*\,E2^3D_2)]\\ &+\cos^2\theta[150|E2^1D_2|^2 - 100|E2^3D_2|^2]\}/\frac{32}{\lambda\!\!\!^{-2}}\frac{d\sigma}{d\Omega}\,.\end{aligned} \tag{2}$$

The differential cross section can be presented as:

$$\frac{d\sigma}{d\Omega} = A[\sin^2\theta(1+\beta\cos\theta+\gamma\cos^2\theta)+\varepsilon\cos\theta+\nu]\,. \tag{3}$$

In the same terms, the cross-section asymmetry of the linearly polarized photon reaction can be represented as follows:

$$\Sigma(\theta) = \frac{\sin^2\theta(1+\alpha+\beta\cos\theta+\gamma\cos^2\theta)}{\sin^2\theta(1+\beta\cos\theta+\gamma\cos^2\theta)+\varepsilon\cos\theta+\nu}. \tag{4}$$

The coefficients A, α, β, γ, ε, and ν are unambiguously connected with multipole amplitudes. As it is obvious from relation (3), only 5 independent coefficients can be calculated in the long-wave approximation using the data on the differential reaction cross-section. So, an improvement in the accuracy of measuring only the differential reaction cross-section gives no way of obtaining information about subsequent multipole amplitudes. In this case, the number of unknown parameters in the right side of eq. (1) would increase much quicker than the number of found coefficients in the left side of the equation. In this connection, in order to obtain information on the succeeding multipole amplitudes, polarization experiments or other data sources are required. As it can be seen from relation (4), the experimental data on the asymmetry of the linearly polarized photon reaction cross-section enable one to calculate the sixth independent coefficient.

It can be demonstrated that on the assumption that $\sigma(E2^3\mathrm{D}_2) \gg \sigma(M1)$, from expressions (1) and (2) we obtain:

$$\alpha = \frac{50|E2^3\mathrm{D}_2|^2}{18|E1^1\mathrm{P}_1|^2 - 9|E1^3\mathrm{P}_1|^2 - 25|E2^3\mathrm{D}_2|^2} > 0\,. \qquad (5)$$

If we assume that $\sigma(M1) \gg \sigma(E2^3\mathrm{D}_2)$, then we have

$$\begin{aligned}\alpha = \; & -18|M1^3\mathrm{D}_1|^2 \\ & +36\sqrt{2}|M1^3\mathrm{S}_1||M1^3\mathrm{D}_1|\cos[\delta(^3\mathrm{S}_1) - \delta(^3\mathrm{D}_1)]\}/ \\ & \{18|E1^1\mathrm{P}_1|^2 - 9|E1^3\mathrm{P}_1|^2 + 9|M1^3\mathrm{D}_1|^2 \\ & -18\sqrt{2}|M1^3\mathrm{S}_1||M1^3\mathrm{D}_1|\cos[\delta(^3\mathrm{S}_1) - \delta(^3\mathrm{D}_1)]\}\,. \qquad (6)\end{aligned}$$

From the phase analysis of elastic (p,^{3}He) scattering Murdoch *et al.* [75] have determined the phase difference to be $\delta(^3\mathrm{S}_1) - \delta(^3\mathrm{D}_1) > 90^0$. Therefore, the both components in the numerator of expression (6) enter with the minus sign, and the coefficient α must be negative.

As a result of the least-squares fit of expressions (3) and (4) to the experimental data on the differential cross section [66] and cross-section asymmetry of linearly polarized photon reactions, the coefficients A, α, β, γ, ε, and ν were calculated [69]. Since the coefficients enter into relations (3) and (4) in linear fashion, the solution was unambiguous.

Since only phase differences enter into formulas (1) and (2), these relations comprise 11 unknown parameters. The currently available experimental data on the (γ, p) and (γ, n) reactions are insufficient for determining all the parameters. According to the experimental data obtained (see Fig.4), α_p and α_n are the minus coefficients, and hence, the least amplitude that enters into expressions (1) and (2) is the E2$^3D_2$ amplitude. After the E2$^3D_2$-comprising components are excluded, expressions (1) and (2) still comprise 9 unknown parameters: $|E1^1P_1|$, $|E2^1D_2|$, $\cos[\delta(^1P_1) - \delta(^1D_2)]$, $|E1^3P_1|$, $|M1^3S_1|$, $|M1^3D_1|$, $\cos[\delta(^3S_1) - \delta(^3D_1)]$, $\cos[\delta(^3S_1) - \delta(^3P_1)]$ and $\cos[\delta(^3P_1) - \delta(^3D_1)]$.

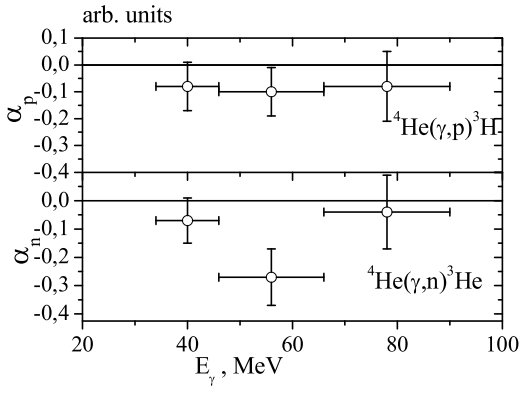

Fig.4. *Coefficients α_p and α_n. The errors are statistical only*

It is known [53] that according to the isospin selection rules for self-conjugate nuclei the isoscalar parts of *E1* and *M1* amplitudes are essentially suppressed. In view of this, using the Watson theorem, the last three phase differences were calculated from the data of phase analysis of elastic (p,^{3}He) scattering [75].

The coefficients A, α, β, γ, ε, and ν are expressed in terms of the multipole amplitudes as:

$$\begin{aligned}A = \lambda^2/32\{&18|E1^1\mathrm{P}_1|^2 - 9|E1^3\mathrm{P}_1|^2 + 9|M1^3\mathrm{D}_1|^2 - \\ &18\sqrt{2}|M1^3\mathrm{S}_1||M1^3\mathrm{D}_1|\cos[\delta(^3S_1) - \delta(^3D_1)]\}; \qquad (7)\end{aligned}$$

$$\begin{aligned}\alpha = \{&-18|M1^3\mathrm{D}_1|^2 + \\ &36\sqrt{2}|M1^3\mathrm{S}_1||M1^3\mathrm{D}_1|\cos[\delta(^3\mathrm{S}_1) - \delta(^3\mathrm{D}_1)]\} \,/\, \frac{32}{\lambda^2}A\,; \qquad (8)\end{aligned}$$

$$\beta = 60\sqrt{3}|E1^1\mathrm{P}_1||E2^1\mathrm{D}_2|\,cos[\delta(^1P_1) - \delta(^1D_2)] \,/\, \frac{32}{\lambda^2}A\,; \qquad (9)$$

$$\gamma = 150|E2^1\mathrm{D}_2|^2 \,/\, \frac{32}{\lambda^2}A\,; \qquad (10)$$

$$\begin{aligned}\varepsilon = \{&-12\sqrt{3}|E1^3\mathrm{P}_1||M1^3\mathrm{D}_1|\,cos[\delta(^3P_1) - \delta(^3D_1)] - \\ &12\sqrt{6}|E1^3\mathrm{P}_1||M1^3\mathrm{S}_1|\,cos[\delta(^3P_1) - \delta(^3S_1)]\} \,/\, \frac{32}{\lambda^2}A\,; \qquad (11)\end{aligned}$$

$$\begin{aligned}\nu = \{&18|E1^3\mathrm{P}_1|^2 + 12|M1^3\mathrm{S}_1|^2 + 6|M1^3\mathrm{D}_1|^2 + \\ &12\sqrt{2}|M1^3\mathrm{S}_1||M1^3\mathrm{D}_1|\,cos[\delta(^3S_1) - \delta(^3D_1)]\} \,/\, \frac{32}{\lambda^2}A. \qquad (12)\end{aligned}$$

The experimentally observable quantities are expressed in terms of multipole amplitudes in a bilinear fashion. Therefore, there must exist two different sets of multipole amplitudes, which satisfy these experimental data. With the help of programs of the least square method (LSM) one positive solution of the problem can be calculated. The second solution can be found, for example, by the lattice method. Since both positive solutions have the same χ^2 values, an additional information is necessary to choose

the proper solution. It should be also noted that if the difference between the solutions is comparable with the amplitude errors, then the LSM errors of the amplitudes may appear overestimated.

The amplitude values were calculated from the derived set of six bilinear equations (7-12) with six unknown parameters using the random-test method [69]. To calculate the errors in the amplitudes, 5000 statistical samplings of A, α, β, γ, ε, and ν values with their errors were performed. The errors in the coefficients were assumed to be distributed by the normal law. After each statistical sampling the set of equations was solved, the calculated amplitude values were stored and then their average values and dispersions were calculated.

According to Ref. [56], one can assume that with the photon energy increase the $M1^3S_1$ transition cross-section decreases as $1/V$, where V is the nucleon velocity. Therefore, at MeV nucleon energies the contribution of the $M1^3S_1$ transition can be neglected. In this connection, out of the two found solutions of the system of equations (7-12) the choice has been made on the solution, where $\sigma(E1^3P_1) > \sigma(M1^3S_1)$.

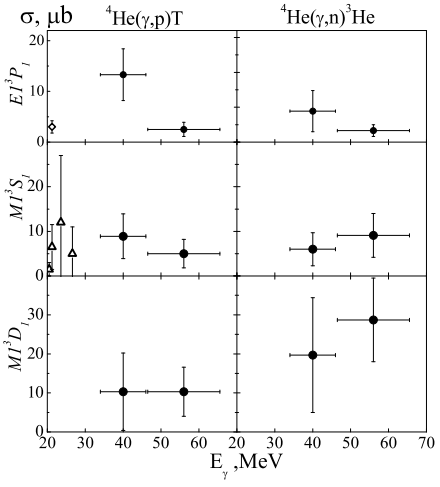

Fig.5. *Total cross sections of spin S=1 transitions of $^4He(\gamma,p)T$ and $^4He(\gamma,n)^3He$ reactions: ◇–data from Ref. [56]; △–data of Ref. [55]; •–data of Ref. [69]. The errors are statistical only*

The findings of the experiment aimed to determine the total cross sections of S=1 transitions are presented in Fig.5. The triangles represent the data of Wagenaar *et al.* [55], the diamond shows the data of Pitts [56] obtained from studies of the reaction of radiative capture of protons by tritium nuclei. The points represent the data of Lyakhno *et al.* [69] from the studies of two-body (γ,p) and (γ,n) reactions of ^{4}He disintegration. The existing experimental data on the total cross-sections of electromagnetic transitions with the spin S =1 in the $^4\mathrm{He}(\gamma,p)\mathrm{T}$ and $^4\mathrm{He}(\gamma,n)^3\mathrm{He}$ reactions have considerable statistic and systematic errors.

If for a certain photon energy range it can be assumed that $\sigma(M1^3S_1) \sim \sigma(E2^3D_2) \sim 0$, then the amount of the available experimental data on the differential cross-section and cross-section asymmetry with linear polarized photons is sufficient for calculating the cross-sections of other transitions with the spin S=1 of the final state of the particle system without invoking the data on elastic (p,^{3}He) scattering.

4. ROLE OF THE SPIN-ORBIT INTERACTION IN NUCLEI

The investigation into the structure of few-nucleon nuclei is of considerable importance for an understanding of the structure of other nuclei. The occurrence of states with nonzero orbital momenta of nucleons in the lightest nuclei is a manifestation of the properties of inter-nucleonic forces and, hence, such effects should be observed without exception in all nuclei as well as in all their excited states.

One can suppose that the contribution of the effects connected with the tensor part of *NN* potential and 3*NF's* increases with a growth of the atomic number. Firstly, it can be seen from the fact that the *D*-state contribution in the deuteron is about 5%, while in the ^{4}He nucleus it makes ∼16%.

Secondly, at the calculation of the probabilities of the outside shell states, for example, in the ^{12}C nucleus, similarly to the case with the ^{4}He nucleus, we must bear in mind that the nucleus spin of ^{12}C can take the values $0 \leq S \leq 6$, the total orbital momentum of the nucleons of ^{12}C can be $0 \leq L \leq 6$, and the orbital momenta of separate nucleons can take on any values, which are not forbidden by the Pauli principle. In other words, the ground state of the nucleus ^{12}C can be of the $^1S_0$, $^3P_0$, $^5D_0$, $^7F_0$, $^9G_0$, $^{11}H_0$, or $^{13}I_0$ states. Nowadays, probability of these states is not held due to their extreme complication. However, the rough estimation of these probabilities can be achieved in the following way. Let us suppose the ^{12}C nucleus consist of three weakly bound α-clusters. The total momentum and parity conservation laws do not forbid, and the tensor part of *NN* interaction and 3*NF's* initiate states with the orbital momenta larger than predicted by the nuclear shell model (NSM) [75, 76] in every cluster, in two clusters at one time or in all three clusters. In the result, the probability of these states in the ^{12}C can be higher than in the ^{4}He nucleus.

Using this supposition one can explain the row of the well-known nuclei properties. Particularly, it is possible to explain the significantly higher contribution of the spin-orbit interaction in the nuclei, than calculated in the NSM frames. Contribution of the spin-orbit interaction A nucleons in the potential energy nucleus can be assessed by the relation:

$$U_{SO} = -\lambda\left(\frac{\hbar}{Mc}\right)^2 \sum_{i=1}^{A} \frac{1}{r_i}\frac{\partial V_i}{\partial r_i}(\vec{l_i}\cdot\vec{s_i})\,, \qquad (13)$$

where M is the nucleon mass, V_i is the spherically symmetrical potential, l is the orbital momentum, s is the spin of the nucleon. However, for the agreement

of the experimental data into the expression (13) was put a constant, which is $\lambda \sim 10$.

The appearance of the fitting constant λ can be partially explained as follows. Let k-number of the nucleons, with the orbital momenta in accordance with the NSM, and other A-k nucleons have orbital momenta bigger than it is predicted by the NSM. Then the expression (13) can be refined as [78]:

$$U_{SO} = -\left(\frac{\hbar}{Mc}\right)^2 \left[\sum_{i=1}^{k} \frac{1}{r_i}\frac{\partial V_i}{\partial r_i} P(l_i^{sh})(\vec{l}_i^{sh} \cdot \vec{s}_i) + \sum_{i=k+1}^{A} \frac{1}{r_i}\frac{\partial V_i}{\partial r_i} P(l_i > l_i^{sh})(\vec{l}_i \cdot \vec{s}_i)\right], \quad (14)$$

where $P(l_i)$ is the probability for the i-th nucleon to have the orbital momentum l_i. The sum of probabilities is $\sum_{i=1}^{A} P(l_i)$=1. Thus, in the case of the lightest nuclei second summing of the expression (14) leads to the small but not equal zero impact of spin-orbit interaction to the potential energy of the nucleus. In medium and heavy nuclei nucleons are situated, generally, in $l > l^{sh}$ states. In other words, the tensor part of NN potential and $3N$ forces push the nucleons outside of nuclear shells, with the rise of atomic number the role of this effects is rising at that. The second summing, which is not predicted by NSM, can give a significant additional contribution to potential energy of a nucleus.

In particular, calculations [79, 80], made on the basis of the Woods-Saxon potential, can give the overestimation of the protons number Z for the position of the island of stability of the superheavy nuclei. In the frames of semiempirical shell models [81] at the extrapolation of fitting expressions for the area of the heavy nuclei to the area of the superheavy nuclei, apparently, the according corrections should be also counted.

5. CONCLUSIONS

Modern methods of the decision of a many-nucleon problem make it possible to calculate the characteristics of few-nucleon nucleus to an accuracy, which is determined by the accuracy the measurement of NN potential, and also $3NF$'s and $4N$ forces. In this connection the ^{4}He nucleus is an ideal laboratory for investigating the properties of these forces.

The measurement of total cross-sections for the electromagnetic transitions with spin S=1 in the final state of the particle system in $^4\mathrm{He}(\gamma, p)^3\mathrm{H}$ and $^4\mathrm{He}(\gamma, n)^3\mathrm{He}$ reactions, and, in addition to data about radiative deuteron-deuteron capture, can possibly allow to separate the effects specified by the nuclear ground state structure from the effects specified by the reaction mechanisms. Theoretical calculations wanted.

The states with non-zero orbital momenta of the nucleons of the lightest nuclei are the manifestation of the properties of inter-nucleonic forces and, consequently, such effects should be observed in all nuclei and in all their excited states. One can suppose, that the tensor part of NN potential and $3N$ forces push the nucleons outside of nuclear shells, with the rise of atomic number the role of these effects is rising at that. This can lead to the additional contribution of the spin-orbital interaction to the potential energy of the nucleus in comparison with an estimation on the nuclear shell model.

Author gives the gratitude to Yu.P. Stepanovsky for important advice and discussion over the article material, and to A.V. Shebeko for the sequence of critical remarks.

References

1. R.W.Woods and D.S.Saxon // *Phys. Rev.* 1954 v. 95, p. 577.
2. J. L.Gammel, R.S.Christian and R.M.Thaler // *Phys. Rev.* 1957, v. 105, p. 311.
3. T.Hamada and I.D.Johnston // *Nucl. Phys.* 1962, v. 34, p. 382.
4. R.V.Jr.Reid // *Ann. Phys.* 1968, v.50, p. 411.
5. M. Lacombe, B. Loiseau, J.M. Richard, R. Vinh Mau, J. Cote, P. Pires, and R.de Tourreil // *Phys. Rev.* 1980, v. C 21, p. 861.
6. R.B. Wiringa, V.G.J. Stoks, and R. Schiavilla // *Phys. Rev.* 1995, v. C 51, p. 38; R.B. Wiringa, S.C. Pieper, J. Carlson,and V.R. Pandharipande // *Phys.Rev.* 2000, v. C 62, p. 014001.
7. R. Machleidt, F. Sammarruca, Y. Song // *Phys. Rev.* 1996, v. C 53, p. R1483; R. Machleidt // *Phys. Rev.* 2001, v. C 63, p. 024001.
8. H. Arenhovel, W. Leidemann, and E. Tomusiak // *Phys. Rev.* 1995, v. C 52, N3, p. 1232.
9. M. Schwamb, H. Arenhoevel // *Phys.Lett.* 2004, v. B588, p. 49.
10. B.S. Pudliner, V.R. Pandharipande, J. Carlson, S.C. Pieper, and R.B. Wiringa // *Phys. Rev.* 1997, v. C 56, p. 1720.
11. S.A. Coon and J.L. Friar // *Phys.Rev.* 1986, v. C 34, p. 1060.
12. J.L. Friar, D. Huber, U. van Kolck // *Phys. Rev.* 1999, v. C 59, p. 53.
13. A. Kievsky, M. Viviani, L. Girlanda, and L.E. Marcucci // *Phys.Rev. 2010, v. C 81, p. 044003.*
14. *K. Sekiguchi, H. Okamura, N. Sakamoto et al.* // Phys.Rev. *2011, v. C83, p. 066001.*
15. *E.J. Brach, O. Hausser, B. Larson, A. Rachav et al.* // Phys.Rev. *1993, v. C47, p. 2064.*
16. *Q. Ye, G. Laskaris, W. Chen, H. Gao et al.* // Eur. Phys. *J.* 2010, v, A44, p. 55.

17. X. Zong, Ph.D. thesis, Department of Physics Duke University, 2010.

18. D.R. Entem and R. Machleidt // *Phys. Rev.* 2003, v. C 68, p. 041001 (R).

19. D. Rozpedzik, J. Golak, R. Skibinski, *et al.* // *Acta Phys.Polon.* 2006, v. B37, p. 2889. e-Print: nucl-th/0606017.

20. G.V. Skornyakov, K.A. Martirosyan // *JETP.* 1956, v. 31, p. 775.

21. L.D. Faddeev // *JETP.* 1960, v. 39, p. 1459.

22. O.A.Yakubovsky // *Yad. Fiz.* 1967, v. 5, p. 1312.

23. W. Gloeckle and H. Kamada // *Nucl. Phys.* 1993, v. A560, p. 541; W. Gloeckle and H. Kamada // *Phys.Rev.Lett.* 1993, v. 71, p. 971.

24. S. Bacca, N. Barnea, W. Leidemann, and G. Orlandini // *Phys.Rev.* 2009, v. C80, p. 064001. e-Print: arXiv:0909.4810 [nucl-th].

25. D. Gazit, S. Bacca, N. Barnea, W. Leidemann, and G. Orlandini // *Phys. Rev. Lett.* 2006, v. 96, p. 112301.

26. M. Viviani, A. Kievsky, and S. Rosati // *Phys.Rev.* 2005, v. C 71, p. 024006.

27. H. M. Hofmann, G. M. Hale // *Phys. Rev.* 2008, v. C77, p. 044002. e-Print: arXiv: nucl-th /0512006v4 (2008).

28. M. Trini, Ph.D. thesis, University of Erlangen-Nurnberg, 2006.

29. H. Kamada, A. Nogga, W. Gloeckle, E. Hiyama *et al.* // *Phys. Rev.* 2001, v. C64, p. 044001.

30. I. Fachruddin, C. Elster, W. Gloeckle // *Mod.Phys.Lett.* 2003, v. A18, p.452; arXiv:nucl-th, 0211069v1, 2002.

31. A. Nogga, H. Kamada, W. Gloeckle, and B.R. Barrett // *Phys. Rev.* 2002, v. C65, p. 054003.

32. A. Nogga, H. Kamada, and W. Gloeckle // *Phys. Rev. Lett.* 2000, v. 85, N5, p. 944.

33. W. Gloeckle, H. Witala, D. Huber, H. Kamada, and J. Golak // *Phys. Rep.* 1996, v. 274, p. 107.

34. J. Kuros-Zolnierczuk, H. Witala, J. Golak, H. Kamada, A. Nogga, R. Skibinski, and W. Gloeckle // *Phys. Rev.* 2002, v. C 66, p. 024003.

35. W. Gloeckle, J. Golak, R. Skibinski, H. Witala, H. Kamada, A. Nogga // *Eur.Phys.J.* 2004, v. A21, p. 335. e-Print: nucl-th/0312006v1.

36. D.O. Riska // *Phys. Scr.* 1985, v. 31, p. 107; 1985, v. 31, p. 471 // *Phys. Rep.* 1989, v. 181, p. 207.

37. A. Amroun, V. Breton, J.M. Caveton *et al.*, // *Nucl. Phys.* 1994, v. A579, p. 596.

38. J. Golak, H. Kamada, H. Witala, W. Gloeckle, J. Kuros-Zolnierczuk, R. Skibinski,V.V. Kotlyar, K. Sagara, and H. Akiyoshi // *Phys. Rev.* 2000, v. C 62, p. 054005.

39. V.V. Kotlyar, H. Kamada, W. Gloeckle,and J. Golak // *Few-Body Syst.* 2000, v. 28, p. 35.

40. R. Skibinski, J. Golak, H. Witala, W. Gloeckle, H. Kamada, A. Nogga // *Phys.Rev.* 2003, v. C67: p. 054002. e-Print: nucl-th/0301051.

41. M. Unkelbach, H.M. Hofmann // *Nucl. Phys.* 1992, v. A 549, p. 550.

42. S. Quaglioni, W. Leidemann, G. Orlandini, N. Barnea, and V. Efros // *Phys. Rev.* 2004, v. C 69, p. 044002.

43. K. Sekiguchi, H. Sakai, H. Witala, W. Gloeckle *et al.* // *Phys. Rev.* 2009, v. C 79, p. 054008.

44. A. Ramazani-Moghaddan-Azani, PhD thesis, University of Gronningen, 2009.

45. V.P. Ladygin, T. Uesaka, T. Saito *et al.* // *Phys. of At. Nucl.* 2006, v. 69, iss. 8, p. 1271.

46. H.R. Weller, P. Colby, N.R. Roberson, and D.R. Tilley // *Phys. Rev. Lett.* 1984, v. 53, p.1325.

47. H.R. Weller, P. Colby, J.L. Langenbrunner, Z.D. Huang, D.R. Tilley, F.D. Santos, A. Arriaga, and A.M. Eiro // *Phys. Rev.* 1986, v. C 34, p. 32.

48. H.R. Weller // *Nucl. Phys.* 1990, v. A508, p. 273.

49. B. Wachter, T. Mertelmeier, and H.M. Hofmann // *Phys. Lett.* 1988, v. B200, p. 246 // *Phys. Rev.* 1988, v. C38, p. 1139.

50. S. Mellema, T.R. Wand, and W. Haeberli // *Phys.Rev.* 1986, v. C 34, p. 2043.

51. J.L. Langenbrunner, G. Feldman, H.R. Weller, D.R. Tilley, B. Wachter, T. Mertelmeier, and H.M. Hofmann // *Phys.Rev.* 1988, v. C38, p. 565.

52. R.M. Whitton, H.R. Weller, E. Hayward, W.R. Dodge, and S.E. Kuhn // *Phys.Rev.* 1993, v. C48, p. 2355.

53. J.H. Eisenberg and W. Greiner. *Excitation Mechanisms of the Nucleus*, in books Nuclear Theory, v. 2, Amsterdam: 1970.

54. K. Sabourov, M.W. Ahmed, S.R. Canon, *et al.* // *Phys.Rev.* 2004, v. C 70, p. 064601.

55. D.J. Wagenaar, N.R. Roberson, H.R. Weller and D.R. Tiller // *Phys. Rev.* 1989, v. C 39, p. 352.

56. W.K. Pitts *Phys. Rev.* 1992, v. C 46, p. 1215.

57. R.S. Canon, S.O. Nelson, K. Sabourov, E. Wulf, H. Weller,*et al.* // *Phys. Rev.* 2002, v. C 65, p. 044008; R.S. Canon, Ph.D. thesis, Duke University, 2001.

58. W. Tornow, J.H. Kelley, R. Raut *et al.* // *Phys. Rev.* 2012, v. C 85, p. 061001(R).

59. A.N. Gorbunov // *Trudy Fiz. Inst. AN SSSR.* (in Russian). 1974, v. 71. p. 3-119.

60. F. Balestra, E. Bollini, L. Busso *et al. Nuovo Cimento.* 1977, v. 38A, p.145.

61. R.T. Jones, D.A. Jenkins, P.T. Deveb et.al. // *Phys. Rev.* 1991, v. C 43, p. 2052.

62. B. Nilsson, J.O. Adler, B.E. Andersson *et al.* // *Phys. Rev.* 2007, v. C 75, p. 014007.

63. T. Shima, S. Naito, Y. Nagai *et al.* // *Phys. Rev.* 2005, v. C72, p. 044004; arXiv:nucl-ex/0509017v1.

64. Yu.M. Arkatov, A.V. Bazaeva, P.I. Vatset *et al.* // *Yad. Fiz.* 1969, v. 10, p. 1123 // *Sov. J. Nucl. Phys.* 1970, v. 10, p. 639.

65. Yu.M. Arkatov, P.I. Vatset, V.I. Voloshscuk *et al.* // *Yad. Fiz.* 1974, v. 19, p. 1172. // *Sov. J. Nucl. Phys.* 1974, v. 19, p. 598 // *Yad. Fiz.* 1971, v. 13, p. 256 // *Yad. Fiz.* 1975, v. 21, p. 925.

66. S.I. Nagorny, Yu.A. Kasatkin, V.A. Zolenko *et al.* // *Yad. Fiz.* 1991, v. 53, p. 365.

67. V.I. Voloshchuk, Dissertation of Doct. Fiz.-Math. Nauk 01.04.16, Kharkov, 1981.

68. Yu.P. Lyakhno, V.I. Voloshchuk, V.B.Ganenko *et al.* // *Yad.Fiz.* 1996, v. 59, p. 18.

69. Yu.P. Lyakhno, I.V. Dogyust, E.S. Gorbenko, V.Yu. Lyakhno, S.S. Zub // *Nucl.Pys.* 2007, v. A 781, p. 306.

70. E.A. Vinokurov, V.I. Voloshchuk, V.B. Ganenko *et al.*// *PAST. Ser. "Jad.-fiz.issled".* Kharkov, 1990, v. 3(11), p. 79.

71. Yu.V. Vladimirov, V.M. Denyak, S.N. Dyukov *et al.* Preprint KhPTI, 89-19, 1989.

72. Yu.P.Mel'nik, A.V. Shebeko. Preprint KhPTI, 84-27, 1984.

73. V.N.Gur'ev. Preprint KhPTI, 71-15, 1984.

74. J.D. Irish, R.G. Johnson, B.L. Berman, B.J. Thomas, K.G. McNeill, and J.W. Jury // *Can. J. Phys.* 1976, v. 53, p. 802.

75. B.T. Murdoch, D.K. Hasell, A.M. Sourkes, W.T.H.van Oers, P.J.T. Verheijen, and R.E. Brown // *Phys.Rev.* 1984, v. C 29, p. 2001.

76. M. Goeppert Mayer, J. Jensen. Elementary theory of nuclear shell structure. New York. USA: John Wiley and Sons. Inc.

77. T. Otsuka, T. Suzuki, R. Fujimoto *et al.* // *Phys. Rev. Lett.* 2005, v. 95, p. 232502.

78. Yu. P. Lyakhno, arXiv:1111.0802v3 [nucl-ex] (2012).

79. F.A. Gareev, B.N. Kalinkin, A. Sobiczewski // *Phys. Lett.* 1966, v. 22, p. 500.

80. R. Smolariczuk // *Phys. Rev.* 1997, v. C 56, p. 812.

81. S. Liran, A. Marinov, N. Zelder // *Phys. Rev.* 2002, v. C 62, p. 024303; arXiv:nucl/th 0102055v1, 2001.

МАЛОНУКЛОННЫЕ СИСТЕМЫ: СОСТОЯНИЕ И РЕЗУЛЬТАТЫ ИССЛЕДОВАНИЯ

Ю.П. Ляхно

Модельно независимые расчёты основных состояний ядер, а также состояний рассеяния можно провести на основе реалистических NN и $3N$ - сил между нуклонами и с применением точных методов решения задачи многих тел. Тензорная часть NN- взаимодействия и $3N$- силы приводят к появлению в легчайших ядрах состояний с ненулевыми орбитальными моментами нуклонов. Эти состояния являются проявлением свойств межнуклонных сил и, поэтому, подобные эффекты должны наблюдаться во всех ядрах и во всех их возбуждённых состояниях. В этой работе большее внимание уделено исследованию ядра ^{4}He.

МАЛОНУКЛОННІ СИСТЕМИ: СТАН І РЕЗУЛЬТАТИ ДОСЛІДЖЕННЯ

Ю.П. Ляхно

Модельно незалежні розрахунки основних станів ядер, а також станів розсіяння можна провести на основі реалістичних NN і $3N$- сил між нуклонами та при застосуванні точних методів вирішення богаточастинкової задачі. Тензорна частина NN- взаємодії і $3N$- сили приводять до появи в основних станах найлегших ядер станів з ненульовими орбітальними моментами нуклонів. Ці стани в найлегших ядрах є проявом властивостей міжнуклонних сил, і тому подібні ефекти повинні спостерігатися у всіх ядрах а також у їх збуджених станах. У цій роботі велика увага приділена дослідженню ядра ^{4}He.